Accepted Manuscript

Title: Theoretical investigation of the thermal performance of a novel solar loop-heat-pipe façade-based heat pump water heating system

Author: Wei He Xiaoqiang Hong Xudong Zhao Xingxing Zhang Jinchun Shen Jie Ji
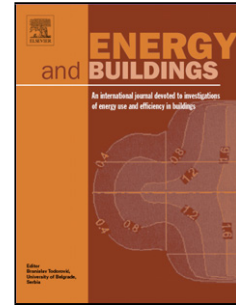
Please cite this article as: W. He, X. Hong, X. Zhao, X. Zhang, J. Shen, J. Ji, Theoretical investigation of the thermal performance of a novel solar loop-heat-pipe façade-based heat pump water heating system, *Energy and Buildings* (2014), http://dx.doi.org/10.1016/j.enbuild.2014.03.053

THEORETICAL INVESTIGATION OF THE THERMAL PERFORMANCE OF A NOVEL SOLAR LOOP-HEAT-PIPE FAÇADE-BASED HEAT PUMP WATER HEATING SYSTEM

Wei He*[1,2], Xiaoqiang Hong[1], Xudong Zhao*[2], Xingxing Zhang[2], Jinchun Shen[2], Jie Ji[1]

[1]Department of thermal Science and Energy Engineering, University of Science and Technology of China,Hefei,China,230026

[2]School of Engineering, University of Hull, Hull, UK, HU6 7RX

*Corresponding author: Tel: +86 551 6360 7390; Fax: +86 551 6360 6459

E-mail: hwei@ustc.edu.cn (Dr. W. He).

Tel: +44 116 257 7971; Fax: +44 116 257 7981

E-mail: xzhao@dmu.ac.uk (Prof. X. Zhao).

Abstract

The aim of the paper was to present a dedicated theoretical investigation into the thermal performance of a novel solar loop-heat-pipe façade based heat pump water heating system. This involved thermo-fluid analyses, computer numerical model development, the model running up, modelling result analyses and conclusion. An energy balance network was established on each part and the whole range of the system to address the associated energy conversion and transfer processes. On basis of this, a computer numerical model was developed and run up to predict the thermal performance of such a system at different system configurations, layouts and operational conditions. It was suggested that the loop heat pipes could be filled with either water, R134a, R22 or R600a; of which R600a is the favorite working fluid owing to its relatively larger heat transfer capacity and positive pressure in operation. Variations in the system configuration, i.e., glazing covers, heat exchangers, would lead to identifiable differences in the thermal performance of the system, represented by the thermal efficiency and COP. Furthermore, impact of the external operational parameters, i.e., solar radiation and ambient air temperature, to the system's thermal performance was also investigated. The research was based on an innovative loop-heat-pipe façade and came up with useful results reflecting the thermal performance of the combined system between the façade and heat pump. This would help promote development and market penetration of such an innovative solar heating technology, and thus contribute to achieving the global targets in energy saving and carbon emission reduction.

Keywords: loop-heat-pipe; façade; heat pump; water heating; building integration; computer modelling.

Nomenclature

A_m	effective module area (m^2)	μ	dynamic viscosity (kg/m-s)
$A_{c,r}$	cross area of refrigerant flow (m^2)	v	viscosity (m^2/s)
$A_{hx,r}$	cross area of refrigerant in heat exchanger (m^2)	ρ	density (kg/m^3)
$A_{hx,s}$	surface area of the plate heat exchanger (m^2)	σ	Stefan- Boltzman constant
C_p	specific heat capacity (J/kg-K)	τ	visual transmittance
D	diameter (m)	χ	vapour quality
g	gravity acceleration (m/s^2)	*Subscripts*	
h	convective heat transfer coefficient (W/m-K)	a	air
h_{fg}	latent heat of vaporization (J/kg)	abs	absorption
h_r	refrigerant heat transfer coefficient (W/m- K)	c	cover
$h_{r,l}$	heat transfer coefficient of liquid refrigerant (W/m- K)	c,c	Condenser coil
h_R	radiative heat transfer coefficient (W/m- K)	c_1	internal cover sheet
H	high (m); thermal enthalpies (J/kg)	c_2	external cover sheet
K	thermal conductivity (W/m^2- K)	d	discharge
k	adiabatic compression index	e	evaportator
l	length (m)	e,t	evaporation thermal energy
m	mass flow rate (kg/s)	f	three-way fitting
n	mesh number; rotation speed (rpm)	g	glazing cover
N	Number	hp	heat pipe
N_{in}	compressor power consumption (W)	hp,e	heat pipe evaporator
Nu	Nusselt number	hp,in	inner heat pipe
Pr	Prandtl number	hp,o	outer heat pipe
p	pressure (pa)	hx	heat exchanger
Q	energy rate (W)	l	liquid
R	thermal resistance (K /W)	L	loss
R_0	universal gas constant (kJ/kmol- K)	m	mean
Ra	Rayleigh number	p	heat pipe wall
Re	Reynolds number	r	refrigerant
t	temperature (^{o}C)	s	solid; isentropic
U	overall heat coefficient (W/m- K)	s,tk	secondary water tank
W	width (m)	th	thermal; theoretical
Greek		tk	primary water tank
α	absorption ratio; thermal diffusivity (m^2/s)	tl	transporting line
β	factor of expansion (K^{-1})	tp	two-phase flow region
δ	thickness (m)	u	useful
ε	Effectiveness (%); porosity	v	vapour; volumetric

η	efficiency		*wi*	wick

1. Introduction

It has been well known that global energy demand is in the trend of continuous growth, and buildings are consuming one third of the total energy supply in developed countries and one fourth in developing countries [1]. Reducing energy demand and making good use of renewable energy are thought to be the major routes towards the low energy and sustainable future, in particular, for the building sector.

Solar technologies have been well developed for many years and are regarded as the most feasible renewable solutions for the building application. Solar thermal, as the most mature technology among all currently available solar technologies, is proven to have relatively higher solar conversion efficiency [2] - two to four times higher than that in solar photovoltaic (PV) systems [3]. Further, solar thermal, owing to the worldwide application and massive scale production, has a much shorter payback period compared to its lifetime. Over the past four decades, solar water heating systems have gained widespread applications in the building sector globally. Most of the solar water heaters were made with flat-plat or heat pipes arrays installed on roofs for layout convenience. This system has been identified with a number of problems that would prevent their promotions, e.g. the installation detracts the aesthetics of the building and requires the long run of water transportation.

In recent years, many façade-based solar water heating systems have been developed and utilized in high-rise building projects, particularly in China. In these systems, the solar collectors (or called 'absorbers') could be fixed to the south-facing balcony of each flat unit [4-6]. This layout can prevent the occupation of the roof space and shortens the distance of pipe runs, and thus enabling improvement of the building's aesthetic effect. However, façade based solar heating systems face a series of challenges: (1) lower solar radiation compared to that on the tilt roof; (2) limited installation area; (3) limited space in kitchen or washroom that may restrict the safe installation of the water tank. All these together may lead to inefficient operation of the system, particularly at high temperature condition.

To overcome the above difficulties, solar heat pump water heating system has been proposed and studied by various researchers [7-11]. This concept could lower the temperature of the solar absorber by controlling evaporation temperature of the refrigerant, and thus improving

the solar efficiency of the system. However, long run of the refrigerant pipes between the outer façade and inside kitchen or washroom may lead to significantly higher refrigerant flow resistance and consequently, power needed for operating the compressor would be increased.

To further improve the performance of the solar water heating systems, a novel loop-heat-pipe (LHP) façade based heat pump water heating system is thereby proposed. The LHP is a two-phase heat-transfer measure with the working fluid circulating across the loop, and thus enabling remote, passive heat transfer at the enhanced capacity. The LHP has been widely ultilized in thermal control of satellites, spacecrafts, electronics and cooling/heating systems [12-13]. Use of LHP for solar energy collection and transportation is the only recent development and still at the research stage. Recent research indicated that LHPs used in the buildings' hot water systems could achieve the enhanced performance if the solar absorber and heat exchanger are adequately selected and coupled [14, 15].

To understand the insights of the innovative LHP façade based heat pump water heating system, a theoretical investigation into the thermal performance of such a system will be carried out by the combined effort of thermo-fluid analyses, computer numerical model development, model running up, modelling result analyses and conclusion. This research will help promote development and market penetration of such an innovative solar heating technology, and thus contribute to achieving the global targets in energy saving and carbon emission in the building sector.

2. System descriptions

The proposed system is schematically shown in Fig. 1, which can be clearly divided into two elements, i.e., outdoor and indoor parts. The outdoor part is a modular package, which receives the solar irradiation and converts it into heat energy in the form of low-temperature vapour. The indoor part consists of a number of components including heat pump compressor, secondary water tank with heat exchanger (heat pipe condenser and heat pump evaporator), expansion valve, primary water tank with embedded heat-exchanging coils (heat pump condenser) and the associated water piping connections, which is designed to gain the solar heat by condensation of the heat pipe vapour, upgrade heat level by heat pump and store this part of heat in the primary water tank for end users.

The outdoor part is a multi-layer façade structure comprising (1) a light weight reinforced polystyrene board acting as the replacement of the existing wall or outer decoration layer of the wall; (2) the parallel-laid capillary tubes made of internally wicked copper pipes, which evenly distribute the working fluid around the inner pipe wall via the wicks, and convert it into vapour upon receiving the solar irradiation casting on the pipes. The tubes are embedded beneath the outer skin with the board by using prefabrication technique, thus enabling merge of the both elements; (3) a thin cooper sheet coated with selective absorption spectrum coating on the outer skin of the board, which acts as the heat absorber and conductor transferring solar heat into the capillary tubes; and (4) a high-solar-transmittance glass cover on the front of the module allowing transmission of the solar radiation into the module and preventing excessive heat loss from the façade surface to the ambient environment.

The indoor part comprises a well-insulated vapour transporting line. Due to the vapour buoyancy, it deliveries the heat from the outdoor vapour header to the indoor secondary water tank with exchanger where the vapour is condensed to a liquid at the same temperature. At the outlet of the secondary water tank where condensed liquid is back to the outdoor part, a fluid reservoir is assembled to adjust the liquid mass participating in the heat transfer process by keeping appropriate liquid mass in fluid reservoir, and it also can stop the penetration of vapour through the pipe. Thus, only the condensed liquid with appropriate mass can flow across and enter the liquid header via a liquid transport line, owing to the gravity caused by the height difference between the exchanger and the liquid header and the system operation pressure varied with the operation temperature. When the solar energy strikes on the south-facing collector surface over the high-solar-transmittance glass cover, the received solar heat converts the working fluid into vapour immediately. Owing to the buoyancy effect of vapour, it will float along the inner space of pipes till the top-level in the vapour header and then flow through well-insulated vapour line into the heat exchanger, which is located inside the secondary water tank. Within the exchanger, the vapour will be condensed into a liquid at the same temperature. The condensed liquid will then flow through a fluid reservoir assembled on the liquid line to the liquid header affected by both the gravity and system operation pressure. After that, this liquid will be evenly scattered to capillary pipes via the three-way feeding at the upper part of each wicked pipe, as showed in Fig. 2.

In addition, there is a heat pump system connecting secondary water tank with primary water tank, the condenser of heat pump is set to be merged in primary water tank, the evaporator of

heat pump is combined with heat exchanger in secondary water tank, then heat pump can enhance the lower temperature water in secondary water tank to higher temperature water in primary water tank according to residents' detailed requirement. Of course, there is feed water inlet and supply water outlet on the primary water tank so that hot water can be supplied to residents at city water pressure. The thermodynamic cycle of the heat pump is shown on a T-S diagram in Fig. 3. Sub-cooled refrigerant, flowing out of the condenser (at point 7), is first throttled in the capillary tube (through the Process 7-8), then enters the heat pump evaporator (at point 8). In the evaporator, the refrigerant absorbs heat from the condensing heat exchanger and vaporizes gradually. The refrigerant becomes slightly superheated at the evaporator output (point 2), and is compressed to a high temperature high pressure superheated gas at the outlet end of the compressor (point 3). Then it discharges the energy in the condenser and becomes a sub-cooled liquid (the process 3-7).

This innovative design allows the combination of solar water heating, LHP technologies, heat pump and heat absorbing pipes in facade, and truly realizes a building-integrated solar heating system with other merits of cost-effective, high efficiency and visually pleasant. The highlights are respectively listed as followings:

(1) The outdoor part is a modular flat unit and embedded into a lightweight board, which could act as a replacement of the current wall structure, or its external decoration layer. This concept will create a building integrated solar water heating system with lower cost.

(2) Loop heat pipes are two-phase heat-transfer devices that separate vapour and liquid flows and thus eliminate the entrainment friction between them, which is one of the major limits impacting on heat pipe heat transfer before. These pipes are therefore able to transfer large amount of heat up to several meters long and keep water pipes from freezing during winter operation.

(3) The secondary water tank is regarded as a temperature bumper, which leads to a gradual temperature variation in the heat exchanger.

(4) A fluid reservoir is set to adjust the liquid mass participating in the heat transfer process, which can reduce the thermal capacity of the outdoor part and react to the solar radiation vary rapidly.

(5) The working fluid in the loop heat pipe is retained at low temperature over the whole operation process, which ensures a constant higher solar efficiency. And the temperature of evaporator in heat pump is higher than a typical water heater with heat pump, which also profits with a higher coefficient performance (COP).

3. Mathematical model and simulations

The simple 1D steady-state model is effective in simulating the performance of the system. So the 1D matrix was considered in this study. The novel façade-based solar water heater system the solar energy conversion and transfer involves three processes, namely: (i) absorbing the certain percentage of solar radiation while remaining being lose into the surrounding air, Q_{th} (ii) transporting the other part of absorbed energy to the heat exchanger of secondary water tank via the loop heat pipe, Q_u (iii) then transporting some part of the energy to(or from while the water temperature in the secondary water tank is higher than the plate heat exchanger) the secondary water tank $Q_{s,tk}$ and transporting the other part of the heat to the passing refrigerant , $Q_{e,t}$, and (iv) upgrading the refrigerant-received heat into higher grade energy using a heat pump. These processes are interconnected and finally can achieve an energy balance among each other under the steady state operation.

3.1 Loop-heat-pipe with solar energy absorber

In operation, solar radiation striking on the absorber will pass across the top cover and be absorbed by the coated surface of the absorbers. Part of the absorbed energy will be dissipated back into the surroundings owing to the directional/diffusive reflection and conductive/convective heat transfer occurring; whereas remaining energy will be absorbed by the heat pipe fluid. Under the steady-state condition, the rate of useful heat equals to the absorbed energy minus the overall heat loss, as showed in Fig. 4.

The useful part of solar energy should be immediately taken away from the absorbers by using the heat pipe loop. This could be achieved by working fluid evaporation in the evaporator section and condensation on the heat exchanger surface in the secondary water tank. In the condensing heat exchanger, the vapour working fluid is condensed and transfers the condensation heat into the product water. Then heat transfer takes place between the heat pump evaporator wall and water in the secondary water tank, thus leading the evaporation of the refrigerant in the evaporator of the heat pump, as depicted in Fig. 5.

The heat balance of the loop-heat-pipe with solar energy absorber part could be expressed as:

$$\tau_g \alpha_c A_m I - U_L A_m (t_p - t_a) = \frac{t_p - t_{hx}}{R_1 + R_2 + R_3 + R_4 + R_5} \tag{1}$$

where I is the solar radiation striking on the panel. So $\tau_g \alpha_c A_m I$ means the solar energy received by the coated fin surface Q_{abs}.

Owing to the temperature difference between the absorber surface and the surrounding air, certain amount of energy will be transferred into the ambient across the top cover. For an absorber surface with the temperature of t_p, by calculating $U_L A_m (t_p - t_a)$ we can get the heat dispersion Q_L from the absorber to the ambient [16, 17], where the U_L is the overall heat transfer coefficient from the absorbers to the ambient across the double-glazed cover top and could be written as:

$$U_L = (\frac{1}{h_{c,\,p\text{-}c2} + h_{R,p-c2}} + \frac{1}{h_{c,\,c2\text{-}c1} + h_{R,c2-c1}} + \frac{1}{h_{c,\,c1\text{-}a} + h_{R,c1-a}}) \tag{2}$$

Assuming a natural convective air layer in existence between the heat pipe absorber and the inner glazing cover, the corresponding heat transfer coefficient can be expressed as [16, 17]:

$$h_{c,p-c2} = \frac{K_{a,p}}{\delta_{a,p}} \left\{ 1 + 1.446(1 - \frac{1708}{Ra_{a,p}\cos\theta})^+ \left[1 - \frac{1708\sin(1.8\theta)^{1.6}}{Ra_{a,p}\cos\theta} \right] + \left[\left(\frac{Ra_{a,p}\cos\theta}{5830} \right)^{0.33} - 1 \right]^+ \right\} \tag{3}$$

$$Ra_{a,p} = \frac{g(t_p - t_{c2})\delta_{a,p}^3}{v_{a,p}^w t_{a,m}} Pr_{a,p} \tag{4}$$

$$t_{a,m} = (t_p + t_{c2})/2 \tag{5}$$

Converting the radiation transfer into the equivalent convective one, a radiation-relevant factor is expressed as [17]:

$$h_{R,p-c2} = \frac{\sigma(t_p + t_{c2})(t_p^2 + t_{c2}^2)}{(1/\xi_p) + (1/\xi_{c2}) - 1} \tag{6}$$

By carrying out a similar analysis, the heat transfer from the inner glazing cover to the

outer glazing cover can be expressed using the equations as followings [17]:

$$h_{c,c2-c1} = \frac{K_{a,c}}{\delta_{a,c}} \left\{ 1 + 1.446(1 - \frac{1708}{Ra_{a,c}\cos\theta})^+ \left[1 - \frac{1708\sin(1.8\theta)^{1.6}}{Ra_{a,c}\cos\theta} \right] + \left[\left(\frac{Ra_{a,c}\cos\theta}{5830} \right)^{0.33} - 1 \right]^+ \right\} \quad (7)$$

$$Ra_{a,p} = \frac{g(t_{c2}-t_{c1})\delta_{a,p}^3}{v_{a,c}^2 t_{c,m}} \text{Pr}_{a,c} \quad (8)$$

$$t_{c,m} = (t_{c1}+t_{c2})/2 \quad (9)$$

$$h_{R,c2-c1} = \frac{\sigma(t_{c1}+t_{c2})(t_{c1}^2+t_{c2}^2)}{(1/\xi_{c1})+(1/\xi_{c2})-1} \quad (10)$$

For convective heat transfer coefficient from a surface exposed to outside wind, it can be calculated using the Klein equation [17]:

$$h_{c,c1-a} = \frac{8.6V^{0.6}}{L^{0.4}} \quad (11)$$

It should be noted that the minimum convective coefficient for wind-exposed surface is considered to be 5W/ (m^2 K); if the calculation of $h_{c,c1-a}$ gives a lower value, this should be used as a minimum.

The radiation heat transfer coefficient is given [17]:

$$h_{R,c1-a} = \xi_{c1}\sigma(t_{c1}+t_a)(t_{c1}^2+t_{c2}^2) \quad (12)$$

Similarly, for the modules with single glazing top cover, the items addressed in equation (7) should be removed, while the heat transfer from inner glazing cover to outer glazing cover will not be counted.

The right part of the expression (1): $\dfrac{t_p - t_{hx}}{R_1 + R_2 + R_3 + R_4 + R_5}$, is the useful part of solar energy transfer from the heat pipe wall to the heat exchanger wall Q_u . This part of heat will eventually be converted into the heat received by the refrigerant and water in the secondary water tank. In that case, the module's thermal efficiency can be defined as:

$$\eta_{th} = \frac{Q_{th}}{A_m I} = \frac{Q_u}{A_m I}$$

(13)

This process involves several thermal resistances, which are the major factors impacting on the magnitude of the loop heat transfer and is detailed as follows.

3.1.1 Thermal resistance of heat pipe wall, R1

Heat transfer through the heat pipe wall is a typical steady-state conduction process, and its thermal resistance can be written as[18]:

$$R_1 = \frac{\ln(D_{hp,o} / D_{hp,in})}{2\pi L_{hp,e} K_{hp} N_{hp}}$$

(14)

3.1.2 Thermal resistance of wick structure, R2

Inner surface of the heat pipe wall is attached with the mesh wick which causes certain resistance in heat transfer; this part of resistance can be written as[18]:

$$R_2 = \frac{\ln(D_{hp,in} / D_{v,e})}{2\pi L_{hp,e} K_{hp} N_{hp}}$$

(15)

$$K_{wi} = \frac{K_l \left[(K_l + K_s) - (1 - \xi_{wi})(K_l - K_s) \right]}{[(K_l + K_s) + (1 - \xi_{wi})(K_l - K_s)]}$$

(16)

$$\xi_{wi} = 1 - \frac{1.05\pi n_{wi} D_{wi}}{4}$$

(17)

where K_{wi} is the effective thermal conductivity of the wick depending upon the porosity of the wick and saturation property of the working fluid.

3.1.3 Thermal resistance of vapour flow, R3

The vapour flow process from the evaporation section to the condensing heat exchanger experiences certain pressure loss and consequently the temperature drop. This creates a resistance in heat transfer which could be written as [13]:

$$R_3 = \frac{t_v^2 R_0 \Delta P_v N_{hp}}{Q_u h_{fg} P_v}$$ (18)

$$\Delta P_v = \Delta P_{v,e} + \Delta P_{v,f} + \Delta P_{v,tl} + \Delta P_{v,hx}$$ (19)

(i) Pressure drop in the evaporator section

$$\Delta P_{v,e} = -\frac{Q_u}{8\rho_v (D_{v,e}/2)^4 h_{fg} N_{hp}}$$ (20)

(ii) Pressure drop in the vapour header

$$\Delta P_{v,f} = -\frac{4\mu_v L_f Q_u}{\pi \rho_v (D_{v,f}/2)^4 h_{fg} N_{hp}}$$ (21)

(iii) Pressure drop in the vapour transportation line

$$\Delta P_{v,tl} = -\frac{4\mu_v L_{tl} Q_u}{\pi \rho_v (D_{v,tl}/2)^4 h_{fg} N_{hp}}$$ (22)

(iv) Pressure drop in the condensation section

$$\Delta P_{v,c} = \frac{4}{\pi^2} \frac{Q_u}{8\rho_v (D_{v,hx}/2)^4 h_{fg} N_{hp}} \frac{1}{(N_{hx}/2)-1}$$ (23)

3.1.4 Thermal resistance of condensed liquid film, R4

The condensed liquid film will be evenly distributed on the surface of the condensing heat exchanger (heat pipe fluid side) and its associated flow resistance is [18]

$$R_4 = \frac{\ln[D_{hx,in}/(D_{hx,in}-2\delta_{lf})]}{2\pi L_{lf} K_{lf}(N_{hx}/2-1)}$$ (24)

3.1.5 Thermal resistance of heat exchanger plat, R5

The equivalent thermal resistance of heat exchanging plate is written as [18]:

$$R_5 = \frac{\ln[D_{hx,o}/D_{hx,in}]}{2\pi(H_{hx}/2)K_{hx}(N_{hx}/2-1)}$$ (25)

3.2 Heat pump system

In this model, the water in the secondary water tank, which leads to mild temperature variation in heat exchanger, will capture or release some part of the energy in the plate heat exchanger, which can be expressed as[18]:

$$Q_{s,tk} = h_{c,w-hx} A_{hx,s} (t_{hx} - t_{s,tk})$$ (26)

$$h_{c,w-hx} = \frac{K_w Nu_{w-hx}}{H_{hx}}$$ (27)

$$Nu_{w-hx} = 0.68 + \frac{0.67 Ra^{1/4}}{[1 + (0.492/\text{Pr})^{9/16}]^{4/9}}$$ (28)

$$Ra_{w-hx} = \frac{g\beta(t_{hx} - t_{s,tk})H_{hx}^3}{\upsilon\alpha}$$ (29)

The other part of heat received by the refrigerant causes its evaporation within the condensing heat exchanger. This refrigerant vapour is then upgraded through a compressor to a high temperature refrigerant vapour, which, in the condenser of the heat pump cycle, is condensed and releases heat to the tank water, resulting temperature rises of the water and condensation of the refrigerant.

The heat received by the refrigerant is given as[19]:

$$Q_{e,t} = m_r A_{c,r}(H_1 - H_4)$$ (30)

Under the steady-state condition, the rate of the useful heat delivered by the loop heat pipe equals to the rate of the energy absorbed by the water in secondary water tank plus the heat received by the refrigerant of heat pump, which could be expressed as:

$$Q_u = Q_{s,tk} + Q_{e,t}$$ (31)

The refrigerant within the heat pump cycle passes across the channels of the plate heat exchanger (refrigerant side) where it is evaporated into vapour. This process involves the turbulent and forced convection heat transfer, which can be written as:

$$u\frac{\partial(\rho_r H_r)}{\partial x} = \frac{\pi D_{hx,in}}{A_{hx,r}} h_r(t_{hx} - t_r)$$ (32)

where H_r is the average specific enthalpy of the refrigerant determined by

$$H_r = xH_v + (1-x)H_l \tag{33}$$

The following expressions can be used to determine the heat transfer coefficient h_r for single-phase flows [20].

$$h_r = \frac{0.023\,\mathrm{Re}^{0.8}\,\mathrm{Pr}^a\,K_r}{D_{hx,in}} \tag{34}$$

where the exponent a is equal to 0.3 for liquid and 0.4 for vapour flow.

The local heat transfer coefficient for two-phase flow is calculated from a correlation, in that [20]

$$h_r = \begin{cases} h_{tp}(x) = 3.4 X_{tt}^{-0.45} h_l, 0 < x \le x_d \\ h_{tp}(x_d) - \left(\dfrac{x-x_d}{1-x_d}\right)^2 \left(h_{tp}(x_d) - h_v\right), x_d < x \le 1 \end{cases} \tag{35}$$

where x_d is the dry-out vapour quality; X_{tt} is the Lockhart-Martinelli parameter which is expressed as [20]:

$$X_{tt} = \left(\frac{\mu_l}{\mu_v}\right)^{0.1} \left(\frac{\rho_v}{\rho_l}\right)^{0.5} \left(\frac{1-x}{x}\right)^{0.9} \tag{36}$$

The authors in a previous study had developed the following compressor model. The mass flow rate m_r of the refrigerant is given by [21]

$$m_r = \frac{\eta_v n V_d}{60 \upsilon_s} \tag{37}$$

where η_v is the volumetric efficiency , n is the rotating speed, V_d is the displacement volume, and υ_s is the specific volume of the refrigerant gas at compressor suction.

The theoretical power consumption and the input power consumption of the compressor are respectively given by [21]

$$N_{th} = \eta_v n V_d P_s \frac{k}{k-1} \left[\left(\frac{P_d}{P_s} \right)^{\frac{k}{k-1}} - 1 \right] \tag{38}$$

and

$$N_{in} = \frac{N_{th}}{\eta_i \eta_m \eta_{mo}} \tag{39}$$

where η_i , η_m and η_{mo} are the indicated efficiency, mechanical efficiency and motor efficiency, respectively.

The refrigerant mass flow rate through the expansion valve can be determined by the following equation [21], at condenser pressure P_c and evaporator pressure P_e,

$$m_r = C_f A_f \sqrt{2 \rho_r (P_c - P_e)} \tag{40}$$

where C_f is the mass flow rate coefficient that depends on the refrigerant density at the valve inlet.

Heat flow of the refrigerant in the condenser coil is the same as equation (32). Because of the difference in the two-phase flow pattern in the evaporator and the condenser, the condensation heat transfer coefficient in two-phase flow region is determined as follows[22],

$$h_{tp} = h_l \left[(1 - x_r)^{0.8} + \frac{3.8 x_r^{0.76} (1 - x_r)^{0.04}}{Pr_r^{0.38}} \right] \tag{41}$$

And heat flow at the immersed condenser coil and the water in primary water tank is described by the following equation [19],

$$Q_c = H_r A_i (t_r - t_{cc}) = H_w (t_{cc} - t_{tk}) \tag{42}$$

The coefficient of performance (COP) of the system could be defined as the ratio of system's

overall heat output and compressor power consumption, as follows [19]:

$$COP = \frac{Q_c}{N_{in}}$$

(4 3)

3.3 Computation method

In this study, numerical simulation with the use of the steady state model was executed to predict the performance of the system when each section of the system finally achieves an energy balance. Fig. 6 gives the flow chart of the computation process for the system. The computer model began with the call for the pre-set external weather conditions, system structure and operating parameters. The simulation included the performance of the loop-heat-pipe and heat pump cycle. The loop-heat-pipe was first computed using the given meteorological data I and t_a to determine the heat pipe wall temperature t_p from an initial guess for the plate heat exchanger temperature t_{hx}. And the computer looped through the compressor, condenser, expansion valve and evaporator (plate heat exchanger) by iteration until a converged solution was obtained. It should be noted that this model was a revised version of the loop-heat-pipe simulation model carried out by Zhao et al. [23, 24] and the heat pump simulation model carried out by Ji et al. [20, 21], which had already been proved with their accuracy for predicting the thermal performance. More detailed descriptions of the above numerical process could be found in Zhao et al. [23, 24] and Ji et al. [20, 21].

4. Results and discussion

The novel LHP heat pump system integrated with building performance was dependent upon its operation and geometrical parameters. In order to evaluate the whole system for different working fluids and different operational parameters, the first set of the LHP in the system is characterized using the dedicated selected parameters shown in Table 1. Table 2 gives the indicative equipment specification of the heat pump in the system being studied, with R134a as the working fluid. The impacts of working fluids used in LHP and impact of the operational parameters (e.g., number of glazing covers, solar radiation, number of flat plate heat exchanger, solar radiation, air temperature) on the system performance were analyzed.

The results were illustrated as below:

4.1 Impact of heat pipe working fluid

Running the above analytical computer model, the results obtained was used to analyse the relationship between the heat transfer performance and the selection of heat pipe working fluid. While remaining the operational parameters constant, change of the working fluid in the heat pipe would lead to the variation of the system heat transfer performance and the results of the simulation were illustrated in Fig. 7. It indicates that the wall temperatures of heat pipe containing refrigerants are higher than that containing water.   Among the refrigerants, the wall temperature of heat pipe that containing R600a is lowest. The useful heat which absorbed by the system that using water as working fluid is higher than that of using refrigerants, and among the refrigerants, using R600a leads to the highest useful energy absorbed. It can be found that by applying water as the working fluid of the LHP, the system can achieve higher solar thermal efficiency and COP. Meanwhile, the use of R600a can obtain higher solar thermal efficiency and COP over R134a and R22 with this particular design.

This phenomenon can be explained as followed: the latent heat of refrigerants was about a tenth of water at the same temperature, and thus enhanced the evaporation rate of the working fluid. Increasing the vapour amount of working fluid flowing in the pipe would create increased pressure drop within the piping, which would consequently lead to increased thermal resistance of vapour flow.   Moreover, water had a relatively larger thermal conductivity than refrigerants, which would consequently result in lower thermal resistance of wick structure and condensed liquid film. The superiority of water enabled the higher amount of heat transported to the heat pump and furthermore, the larger amount of refrigerant mass flow rate within the heat pump would increase the convective heat transfer coefficient. Apparently, water could give a better thermal performance compared with these refrigerants.

The final choice of the working fluid for the loop heat pipe was R600a. A favorite working fluid in the LHP heat pump system should be of characteristics of not only good thermophysical properties, which allowed a large amount of heat to be conducted from the outdoor part to the indoor part with minimum fluid flow, but also the proper vapour pressure

over the operating temperature range. As the vapour pressure of water at the operating temperature was far below standard atmospheric pressure, it needs evacuation while filling the water into the heat pipe. However, refrigerants allowed the loading process carried out under atmospheric pressure. As we can see from the results listed above, R600a is the most preferable option for the heat pipe working fluid compared with R134a and R22.

4.2 Impact of the top glazing covers

The efficiency of the system would also depend upon the number of the top glazing covers. Varying the layer of the top glazing covers from 0 to 2 while remain the above system structure and operating conditions constant, simulation was carried out using the established computer programme, and the results of the simulation were illustrated in Fig. 8. It indicates that increasing the number of the glazing cover led to increase in the thermal efficiency (from 25.90% to 44.7%) and in the system's COP (from 3.69 to 5.27). The increasing percentage of the thermal efficiency and system's COP were found to be 51.5% and 28.8% when increasing the number of glazing covers from 0 to 1, while these to be 14.0% and 10.8% when increasing the number of glazing covers from 1 to 2.

This phenomenon is mainly due to more glazing covers helped reduce the heat transfer between ambient and heat pipe, thus leading to higher thermal efficiency and system's overall performance coefficient. The final choice for the system was the single glazing cover as it could minimize heat loss and reduce the weight of the module for safety which was very important for the façade-based system.

4.3 Impact of plate heat exchanger

Theoretically, more heat exchangers would lead to enhancing the heat transfer between the heat pipe condensing fluid on one side of the heat exchanging plate and heat pump evaporating fluid flow across the other side and therefore, enhanced heat output in terms of solar energy conversion. Varying the number of the plate heat exchangers between LHP and heat pump from 1 to 3 while remaining other parameters constant, simulation was carried out using the established computer programme, and the results of the simulation were shown in Fig. 9. It is found that applying more plate heat exchangers decreased the temperature at heat pipe wall (from 62.8 ^{o}C to 55.6 ^{o}C), while enabled increased solar thermal efficiency (from

39.25% to 47.3%), and enhanced the system's overall performance (from 4.76 to 5.36). The increasing percentage of the thermal efficiency and system's COP were found to be 17.1% and 10.8% when increasing the number of plate heat exchanger from 1 to 2, while these to be 2.9% and 1.6% when increasing the number of glazing covers from 2 to 3.

However, it should be noted that the more the plate heat exchangers used, the more refrigerants need to be filled in the system. While we just only considered the heat transfer characteristic of the system, the impact of the filling amount of refrigerants filled in the heat pump would be taken into consideration in the dynamic model.

4.4 Impact of external parameters

The system's thermal performance would vary with the external parameters, i.e., solar radiation and ambient air temperature. Varying the solar radiation from 200 to 800 W/m2 while remaining other parameters constant, simulation was carried out using the established computer programme. Varying the ambient air temperature from $10\,^{o}C$ to $30\,^{o}C$ while remain the other parameters constant, simulation was carried out. The results of the simulation were shown in Fig. 10 and Fig. 11. It is found that increasing the solar radiation led to significant increase in temperature at heat pipe wall (from $35.3\,^{o}C$ to $75.4\,^{o}C$) and in heat pump's COP (from 2.68 to 5.46), and decrease in thermal efficiency (from 42.2% to 38%). However, under certain solar radiation, the thermal efficiency (from 35.0% to 43.6%) and COP (from 4.50 to 5.01) would increase when the ambient temperature increased. The phenomena could be explained as follows: a higher solar radiation yielded an enhanced solar heat transfer, which would help increases the evaporating temperature thus improves system's COP. Meanwhile, the increasing of the temperature of the heat pipe wall would increase the heat loss thus leading to decrease in thermal efficiency. Having fixed up solar radiation, the higher ambient air temperature reduced the module's heat loss and increased the heat pump evaporating temperature, resulting in increase in the system's thermal efficiency and COP. Since higher levels of solar radiation and ambient temperature are favourable to the COP, using various compressor speed design is the preferable option in the system.

5. Conclusion

Based on an innovative loop-heat-pipe façade and its combination with a heat pump for use

in water heating, a theoretical investigation into the thermal performance of such a system was carried out by the combined effort of thermo-fluid analyses, computer numerical model development, model running up, modelling result analyses and conclusion. This research would help understand the insights, promote development and market penetration of such an innovative solar heating technology, and hence contributed to achieving the global targets in energy saving and carbon emission in the building sector.

In terms of the working fluids, water, R600a, R134 and R22 were applicable for use in the heat pipe loop. Of those, water presented the highest heat transfer capacity but required the lowest pressure (below the atmospheric pressure), which may create a certain level of difficulty in operation, especially for large scale building application. R600a, with the second largest heat transfer capacity and positive operational pressure (above the atmospheric pressure), was considered the most favorite fluid for use in building scale loop heat pipe.

In terms of the system configuration, glazing cover and heat exchanger were the important factors impacting on the thermal performance of the system. Increasing the number of the glazing covers led to the increase of the solar absorber's thermal efficiency and the COP of the whole system. Considering the balance of the economy, safety and efficiency, single-glazed-cover may be a good choice for the façade based solar system application. Increasing heat transfer area of the heat exchanger, the solar absorber's thermal efficiency and the system's COP would initially rise up quickly.

External parameters including ambient temperature and solar radiation also had impact on the thermal performance of the system. Higher ambient temperature led to reduce heat loss from the solar absorber to the surrounding, and hence enhanced solar thermal efficiency of the absorber and COP of the whole system. Similarly, higher solar radiation helped improve the thermal efficiency of the solar absorber as well as the COP of the whole system.

It should be stressed that the paper has only reported the theoretical study of the system that was the first stage of the research. Follow-on works including system prototype construction, laboratory-based measurement, and model validation/modification will be reported in the subsequent paper.

Acknowledgements

References

[1]. M. Wall, M. C. M. Probst, C. Roecker, M. C. Dubois, M. Horvat, O. B. Jorgensen, K. Kappel, Achieving Solar Energy in Architecture - Iea Shc Task 41, 1st International Conference on Solar Heating and Cooling for Buildings and Industry (Shc 2012) 30 (2012) 1250-1260.

[2]. Probst MCM. Architectural integration and integration design of solar thermal systems [Internet]. PhD thesis of ÉCOLE POLYTECHNIQUE FÉDÉRALE DE LAUSANNE. 2008 [cited 2013 Apr 18]. Available from: http://www.bisolnet.ch/Munari%20Probst-final.pdf

[3]. P. Pinel, C. A. Cruickshank, I. Beausoleil-Morrison, A. Wills, A Review of Available Methods for Seasonal Storage of Solar Thermal Energy in Residential Applications, Renewable & Sustainable Energy Reviews 15 (2011) 3341-3359

[4]. V. Badescu, B. Sicre, Renewable Energy for Passive House Heating Part I. Building Description, Energy and Buildings 35 (2003) 1077-1084.

[5]. H. Gunerhan, A. Hepbasli, Exergetic Modeling and Performance Evaluation of Solar Water Heating Systems for Building Applications, Energy and Buildings 39 (2007) 509-516.

[6]. Q. Zhai, R. Z. Wang, Y. J. Dai, J. Y. Wu, Y. X. Xu, Q. Ma, Solar Integrated Energy System for a Green Building, Energy and Buildings 39 (2007) 985-993.

[7]. T. L. Freeman, J. W. Mitchell, T. E. Audit, Performance of Combined Solar-Heat Pump Systems, Solar Energy 22 (1979) 125-135.

[8]. Y. W. Li, R. Z. Wang, J. Y. Wu, Y. X. Xu, Experimental Performance Analysis and Optimization of a Direct Expansion Solar-Assisted Heat Pump Water Heater, Energy 32 (2007) 1361-1374.

[9]. H. Li, H. X. Yang, Potential Application of Solar Thermal Systems for Hot Water Production in Hong Kong, Applied Energy 86 (2009) 175-180.

[10]. T. T. Chow, G. Pei, K. F. Fong, Z. Lin, A. L. S. Chan, M. He, Modeling and Application of Direct-Expansion Solar-Assisted Heat Pump for Water Heating in Subtropical Hong Kong, Applied Energy 87 (2010) 643-649.

[11]. A. Caglar, C. Yamali, Performance Analysis of a Solar-Assisted Heat Pump with an Evacuated Tubular Collector for Domestic Heating, Energy and Buildings 54 (2012) 22-28.

[12]. Faghri A, Heat pipe science and technology, 1st ed., Taulor & Francis Group,1995.

[13]. Dunn PD, Reay DA, Heat pipes, 4th ed., Elsevier Science Ltd.,1994.

[14]. Z. Wang, Z. Duan, X. Zhao, M. Chen, Dynamic Performance of a Facade-Based Solar Loop Heat Pipe Water Heating System, Solar Energy 86 (2012) 1632-1647.

[15]. S. B. Riffat, X. Zhao, P. S. Doherty, Developing a Theoretical Model to Investigate Thermal Performance of a Thin Membrane Heat-Pipe Solar Collector, Applied Thermal Engineering 25 (2005) 899-915.

[16]. Duffle JA, Beckman WA, Solar engineering of thermal processes. 2nd ed., New York: John Wiley and Sons Inc., 1991.

[17]. Kalogirou Soteris A, Solar energy engineering: process and system, Elsevier Inc., 2009.

[18]. Rohsenow W, Harnet J, Cho Y, Handbook of heat transfer, 3rd ed., McGraw-Hill, 1998.

[19]. Turns Stephen T, Thermodynamics: concepts and applications, Cambridge University Press, 2006.

[20]. J. Ji, K. L. Liu, T. T. Chow, G. Pei, W. He, H. F. He, Performance Analysis of a Photovoltaic Heat Pump, Applied Energy 85 (2008) 680-693.

[21]. J. Ji, H. F. He, T. Chow, G. Pei, W. He, K. L. Liu, Distributed Dynamic Modeling and Experimental Study of Pv Evaporator in a Pv/T Solar-Assisted Heat Pump, International Journal of Heat and Mass Transfer 52 (2009) 1365-1373.

[22]. Shah, M.M., A general correlation for heat transfer during film condensation inside pipes, International Journal of Heat and Mass Transfer 22 (1979) 547-556.

[23]. X. X. Zhang, X. D. Zhao, J. H. Xu, X. T. Yu, Characterization of a Solar Photovoltaic/Loop-Heat-Pipe Heat Pump Water Heating System, Applied Energy 102 (2013) 1229-1245.

[24]. X. D. Zhao, Z. Y. Wang, Q. Tang, Theoretical Investigation of the Performance of a Novel Loop Heat Pipe Solar Water Heating System for Use in Beijing, China, Applied Thermal Engineering 30 (2010) 2526-2536.

List of Figures captions

Table 1: Design parameters of the LHP operation and heat exchanger

Parameters	Nomenclature	Value	Unit
External diameter of evaporator	$D_{hp,o}$	0.016	m
Internal diameter of evaporator	$D_{hp,in}$	0.015	m
Thermal conductivity of evaporator wall	K_{hp}	394	w/m-K
Evaporator length	$L_{hp,e}$	1.2	m
Internal diameter of three-way feeding	$D_{v,f}$	0.014	m
Evaporator-to-condenser height difference	H_{hx-hp}	0.25	m
Liquid filling level	m_f	35	%
Transportation line outer diameter	$D_{ltl,o} / D_{vtl,o}$	0.032	m
Transportation line inner diameter	$D_{ltl,in} / D_{vtl,in}$	0.029	m
Transportation line length	L_{ltl} / L_{vtl}	1.0/1.2	m
Wire diameter (wick layer I)	$D_{owi,ms}$	7.175×10^{-5}	m
Layer thickness (wick layer I)	$\delta_{owi,ms}$	3.75×10^{-4}	m
Mesh number (wick layer I)	$n_{owi,ms}$	6299	/m
Wire diameter (wick layer II)	$D_{iwi,ms}$	12.23×10^{-5}	m
Layer thickness (wick layer II)	$\delta_{iwi,ms}$	3.75×10^{-4}	m
Mesh number (wick layer II)	$n_{iwi,ms}$	2362	/m
Wick conductivity	$K_{s,ms}$	394	w/m-K
Numver of heat pipes	N	10	-
Heat exchanger plate thickness	δ_{hx}	0.0024	m
Heat exchanger plate height	H_{hx}	0.289	m
Heat exchanger plate cluster width	W_{hx}	0.318	m
Heat exchanger plate cluster length	L_{hx}	0.119	m
Heat exchanger plate conductivity	K_{hx}	16.28	w/m-K
Heat exchanger number of plate	n_{hx}	140	-
Volume of the secondary water tank	$V_{s,tk}$	30	L

Table 2: Design parameters of the heat pump

Parameters	Nomenclature	Value	Unit
Rated input power of compressor	$N_{in,rated}$	0.25	HP
Diameter of immersed coil in condenser	D_{cc}	9.52	mm
Thickness of the immersed coil	δ_{cc}	1.00	mm
Length of the immersed coil	L_{cc}	4	m
Volume of the primary water tank	V_{tk}	150	L

Fig1 ACCEPTED MANUSCRIPT
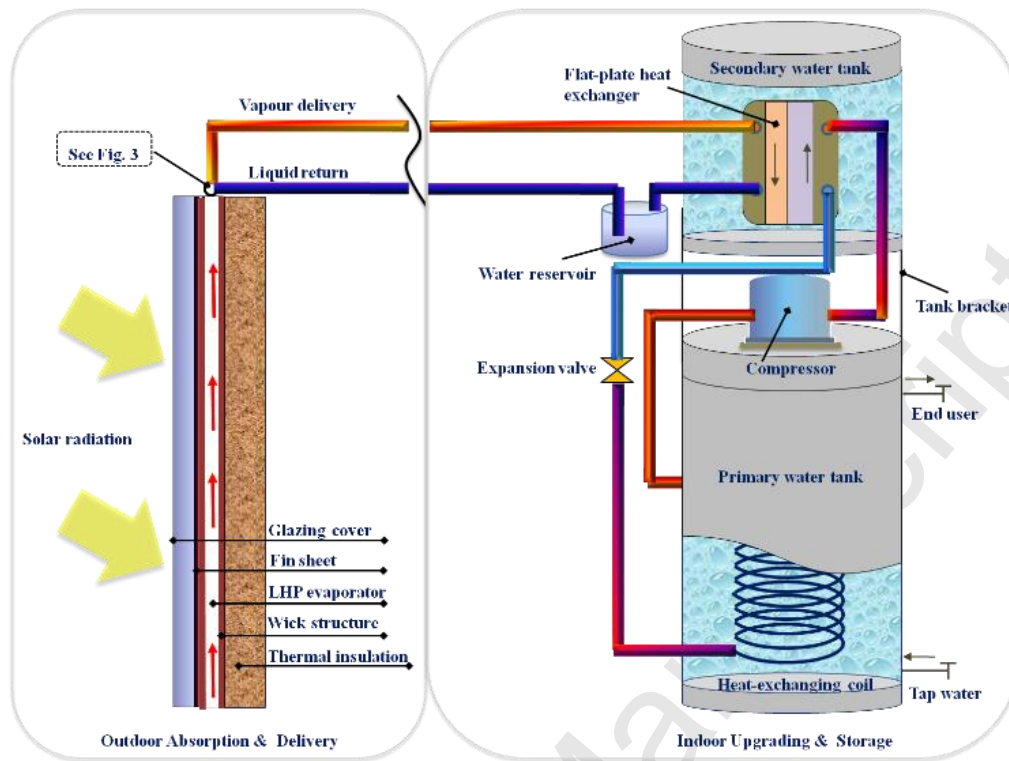
Fig. 1: Schematics of the novel solar loop-heat-pipe water heating system
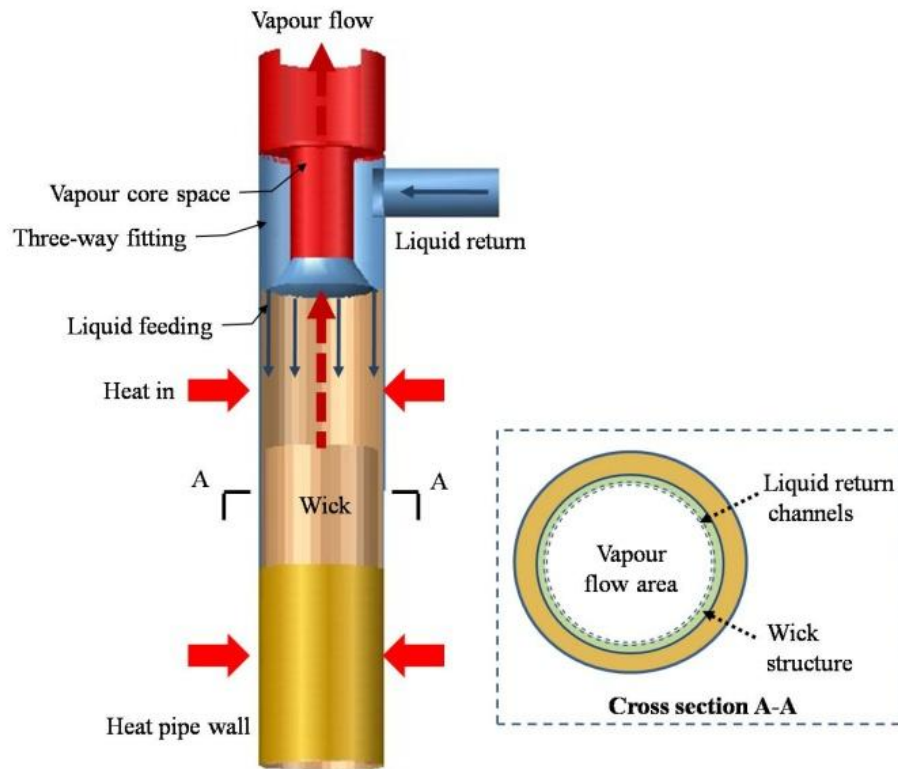
Fig2

Fig. 2: Schematic of three-way feeding and vapour/liquid separation structure
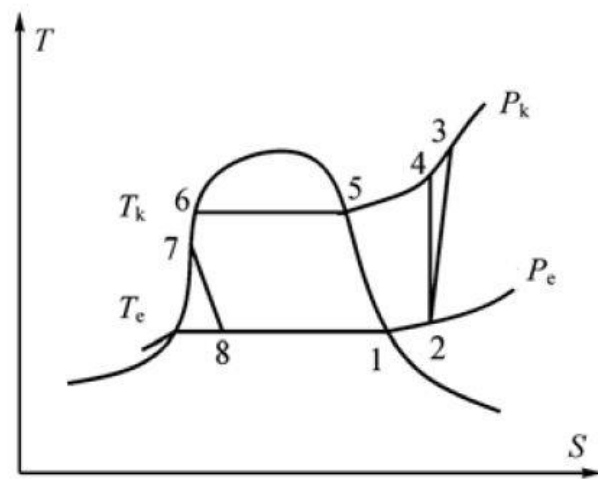
Fig3

T_k: condensing temperature, °C; T_e: evaporating temperature, °C;
P_k: condensing pressure, Pa; P_e: evaporating pressure, Pa

Fig. 3: heat pump thermodynamic cycle in T-S chart
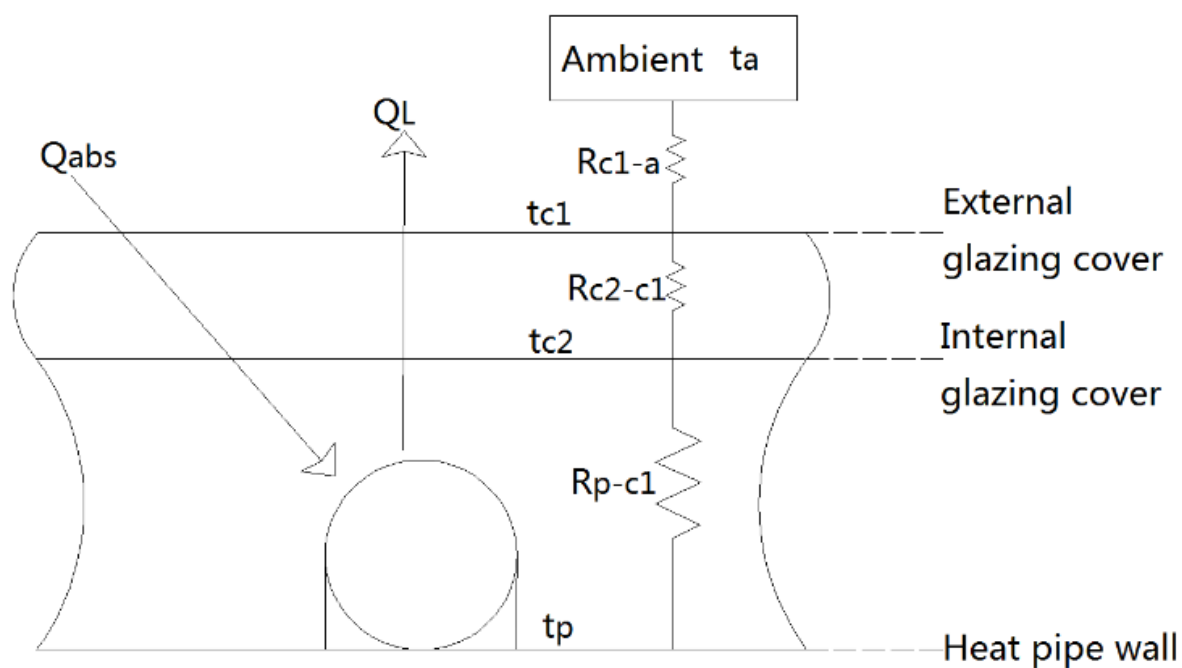
Fig4

Fig. 4: Schematic of heat transfer within the absorber
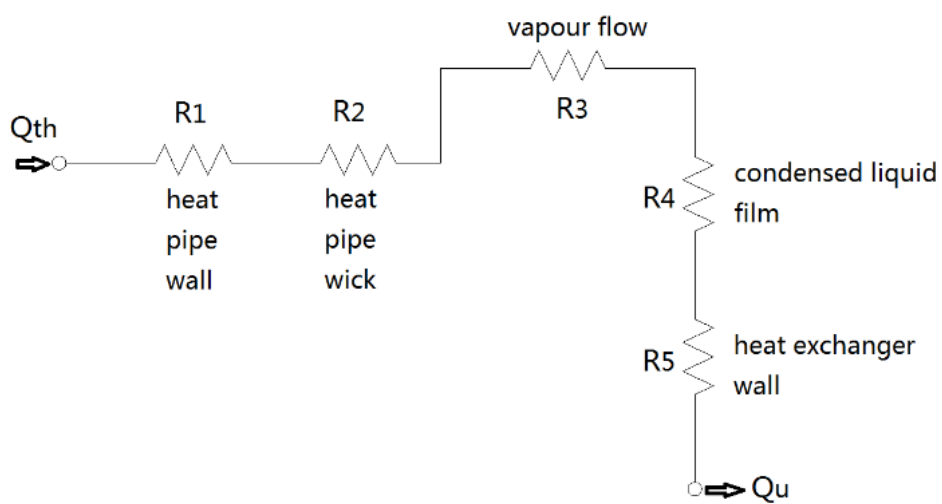
Fig5

Fig. 5: Schematic of heat transfer along the loop-heat-pipe
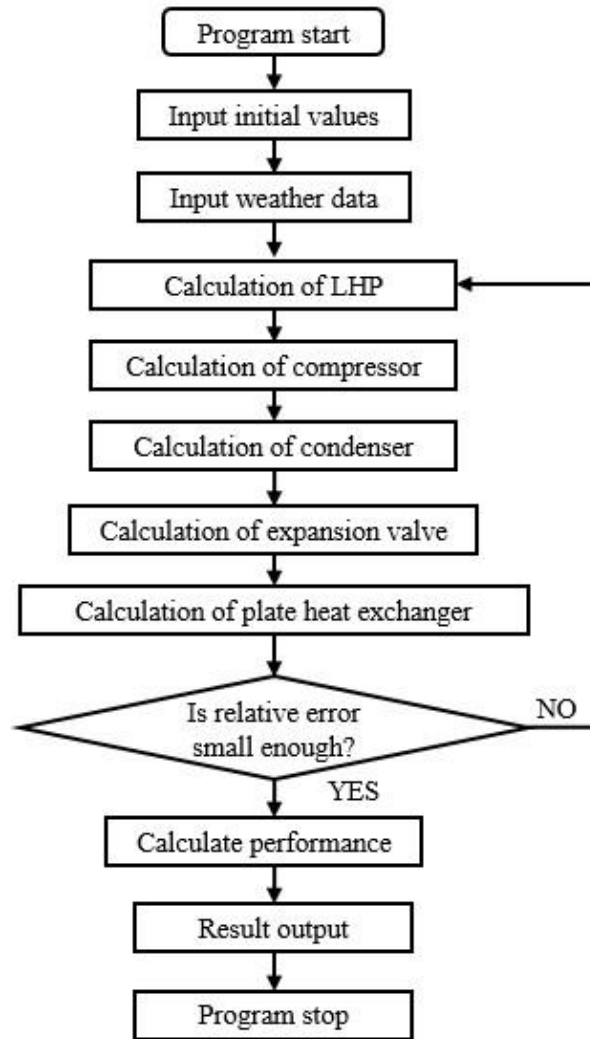
Fig. 6: Flow chart of the computation process for the system model
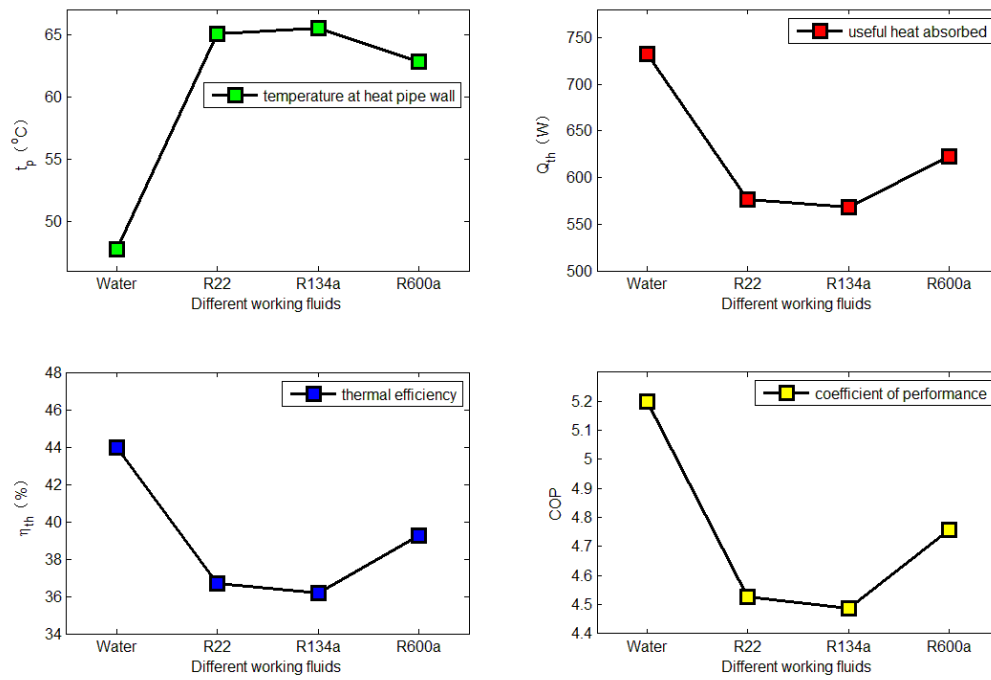
Fig. 7: Temperature at heat pipe wall, useful energy absorbed by LHP, module thermal efficiency and COP as a function of different working fluids
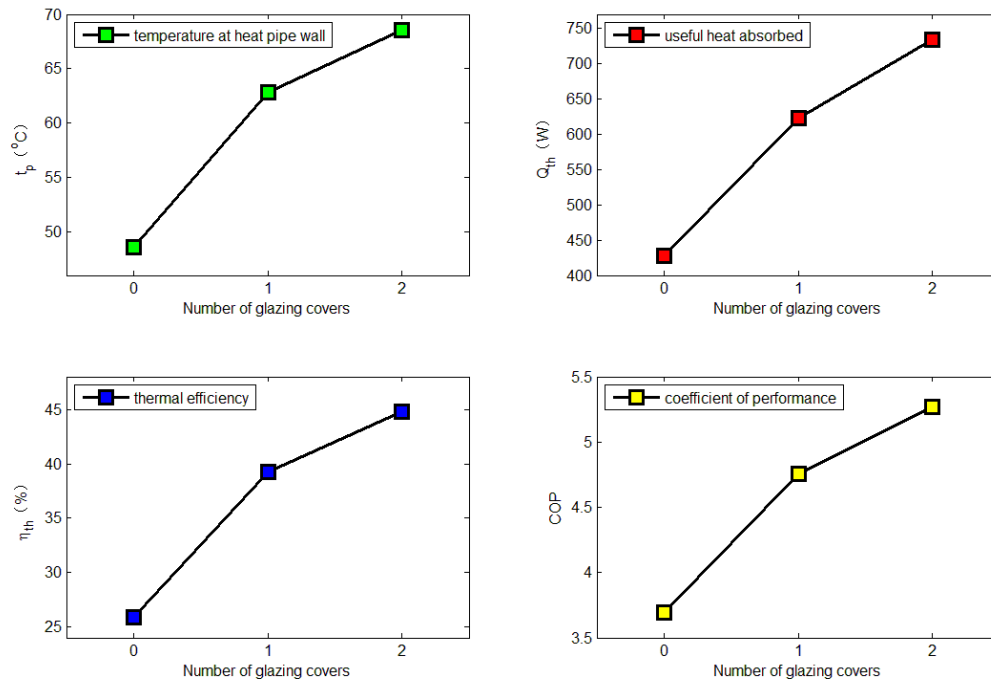
Fig. 8: Temperature at heat pipe wall, useful energy absorbed by LHP, module thermal efficiency and COP as a function of number of glazing covers
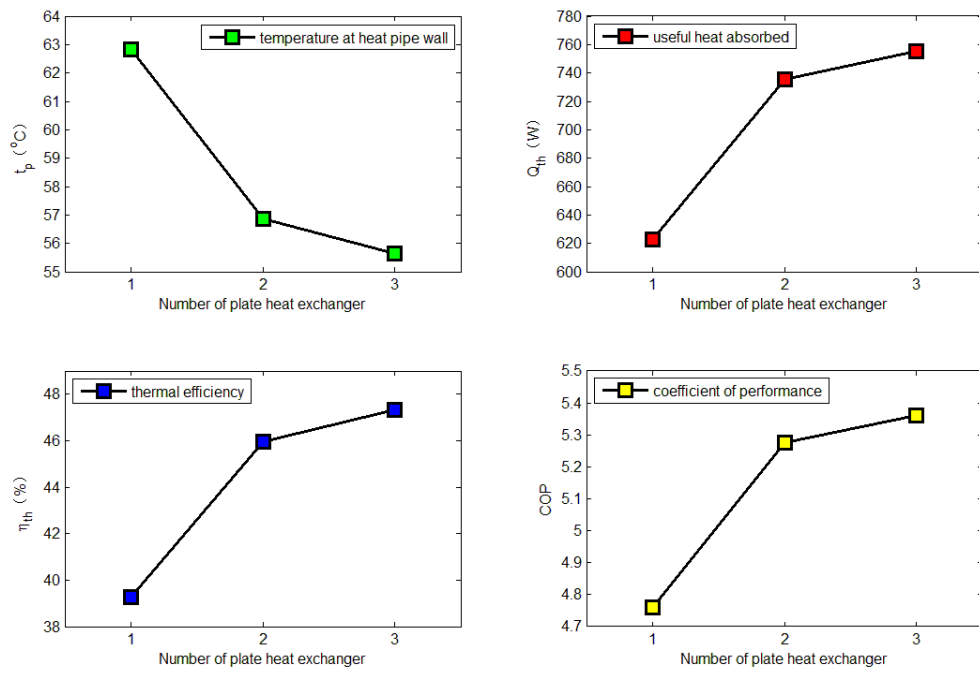
Fig. 9: Temperature at heat pipe wall, useful energy absorbed by LHP, module thermal efficiency and COP as a function of number of plate heat exchanger
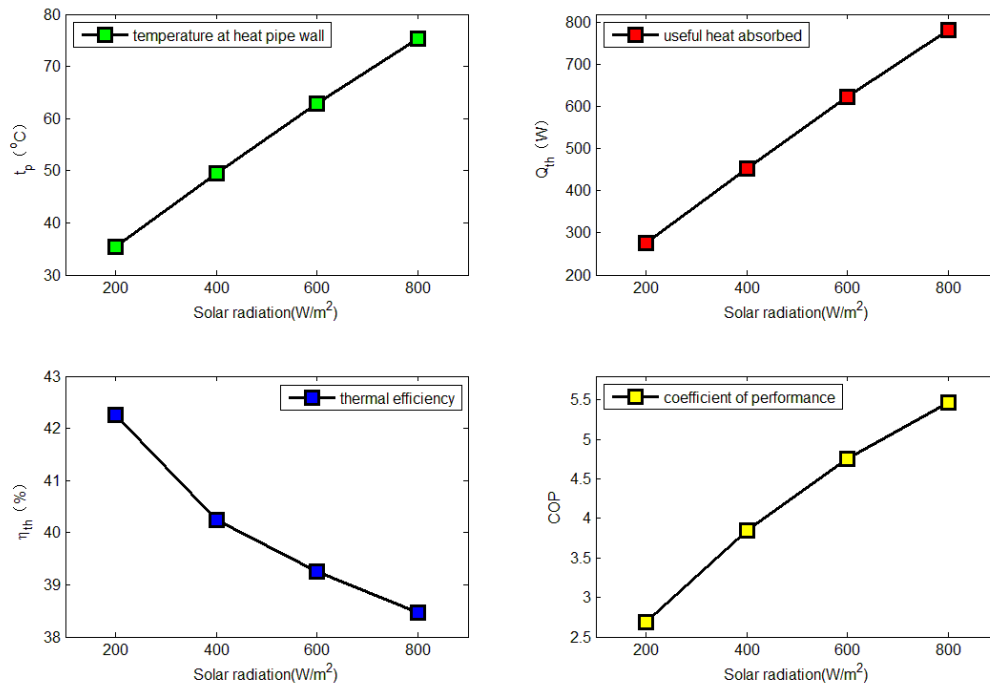
Fig10

Fig. 10: Temperature at heat pipe wall, useful energy absorbed by LHP, module thermal efficiency and COP as a function of solar radiation
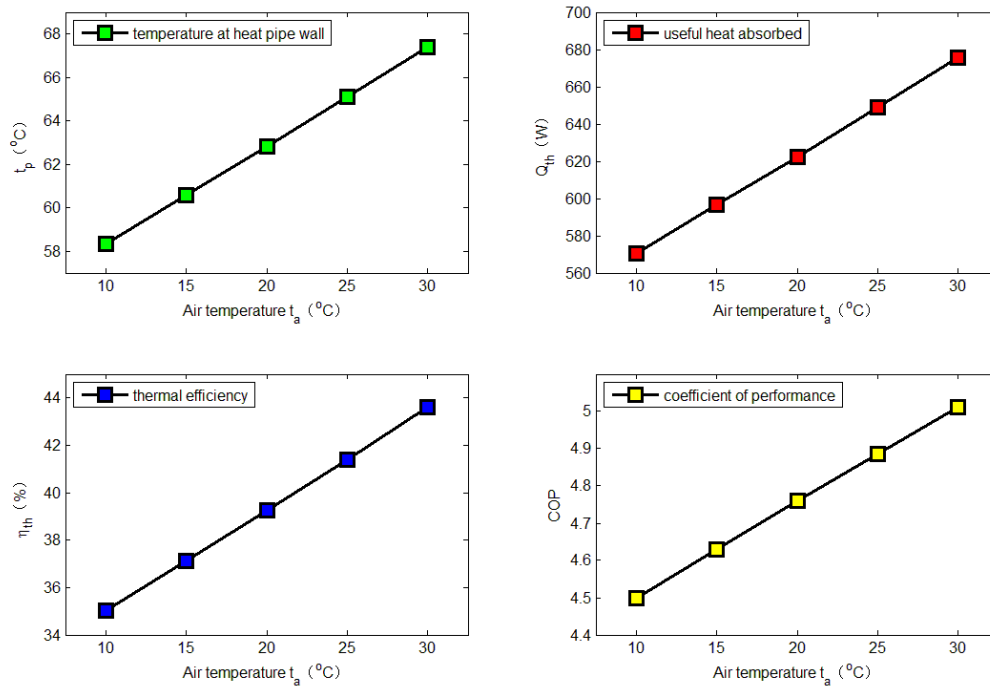
Fig. 11: Temperature at heat pipe wall, useful energy absorbed by LHP, module thermal efficiency and COP as a function of air temperature

- A novel solar loop-heat-pipe façade based heat pump water heating system is described.
- A dedicated theoretical investigation into the thermal performance of the system is presented.
- R600a is suggested to be the favorite working fluid that filled in the Loop Heat Pipes compared to water, R134a and R22.
- The impacts of the system configuration and external parameters are explored.